脈動実体波を使って地球内部構造を探る

西田究 (東京大学地震研究所)

Microseisms excited by ocean swell

- Primary microseisms (0.05-0.1 Hz): smaller
- Secondary microseisms (0.1-0.5 Hz): larger
  - Wiechert 1904
- Excitation mechanism: ocean swell
- Ocean swell: 0.05-0.2 Hz phase velocity～20m/s
  - Longuet-Higgins 1950

Microseisms

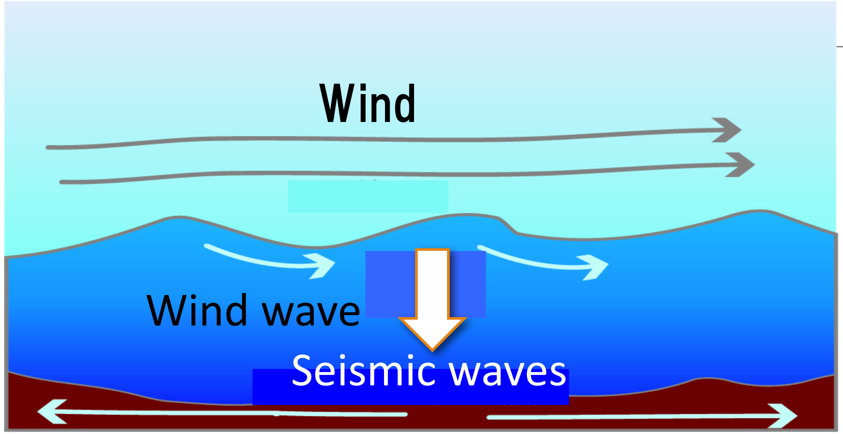

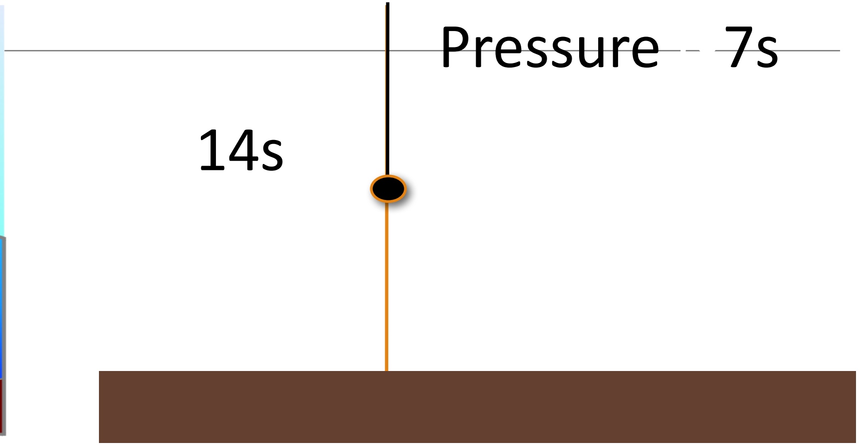

Kedar et al., 2008

- Double frequency microseisms (~7s)
  - excited by Ocean swell (period ~ 14 s)
  - Single force on the sea surface (Longuet-Higgins mechanism)
  - Dominance of Rayleigh waves

Body-wave microseisms

J. Zhang et al. / Earth and Planetary Science Letters 292 (2010) 419–427 421

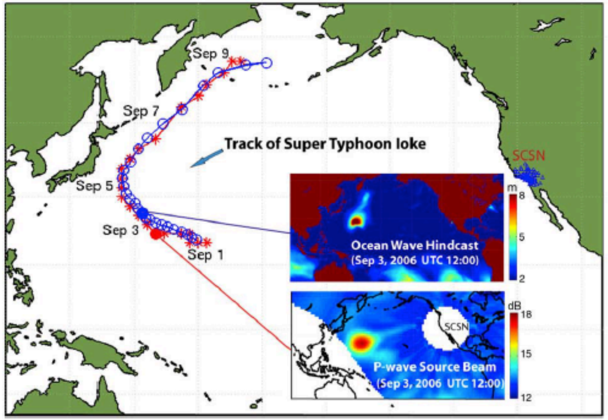

Fig. 2. Tracks of the *P*-wave source regions (stars) and Super Typhoon Ioke (circles). The track points of the peaks of source regions are derived from source beamforming using the SCSN seismic data (every 6 h, and limited by the 2° resolution). The best track of Super Typhoon Ioke is based on the observations and analysis of the Japan Meteorological Agency and available from [http://agora.ex.nii.ac.jp/digital-typhoon/]. The inserts show both a map of the ocean wave hindcast and a map of the *P*-wave source region, sampled for September 3, 2006, UTC 12:00.

Zhang et al. 2010

- Recently teleseismic body-wave microseisms has been focused
  - e.g. Gerstoft et al. 2008, Gualtieri et al. 2013
- Body wave has rich information of the sources
  - Source locations
- Energy partition between P and S waves can constrain the source mechanism

Microseisms from a weather bomb

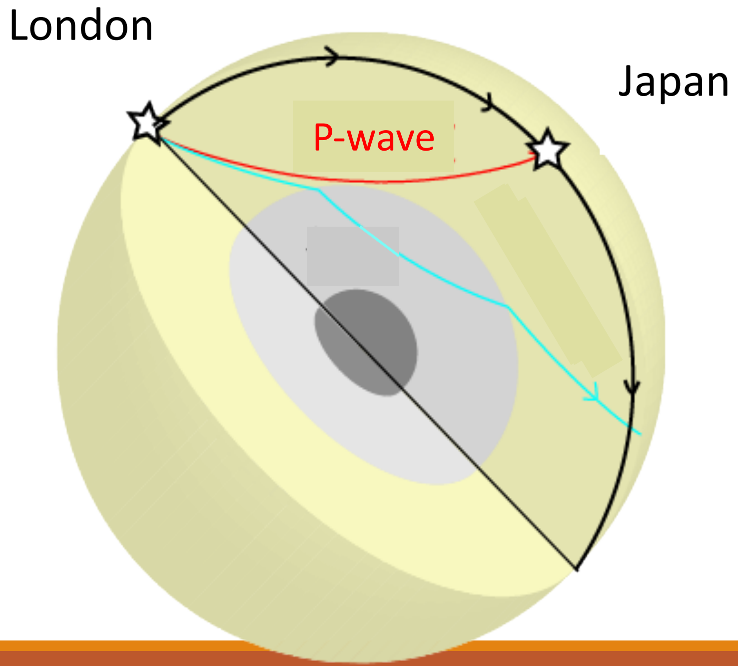

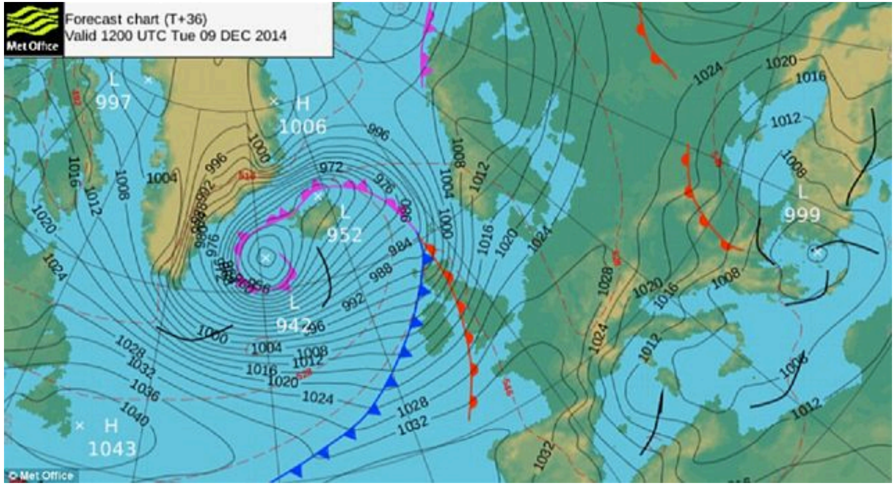

A weather bomb in the Atlantic ocean

- 9th-10th December 2014.

遠くの嵐: 爆弾低気圧(大西洋)

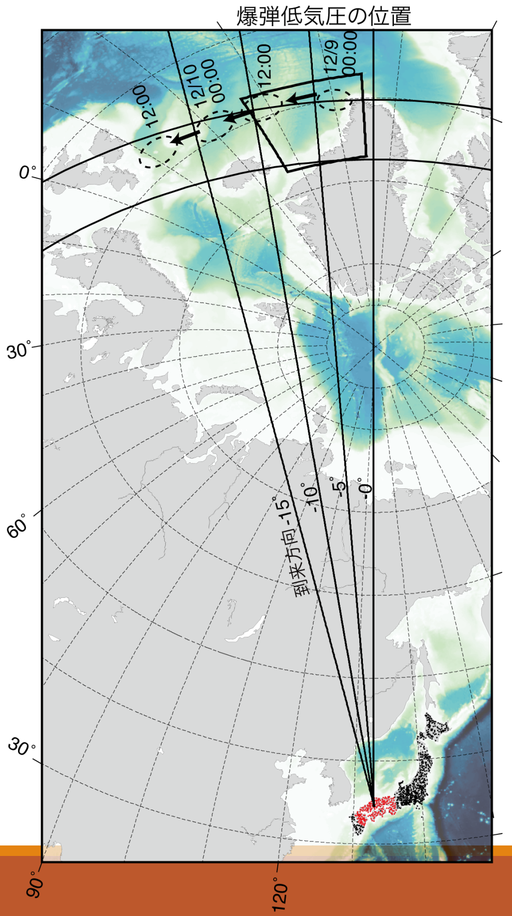

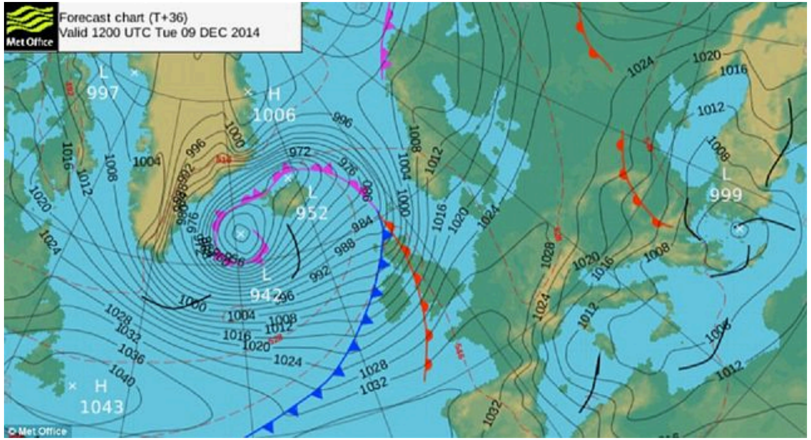

- 大西洋で2014年12月9日に爆弾低気圧発生時
  - イギリスやアイルランドに被害
- 日本の地震計データを解析

Data

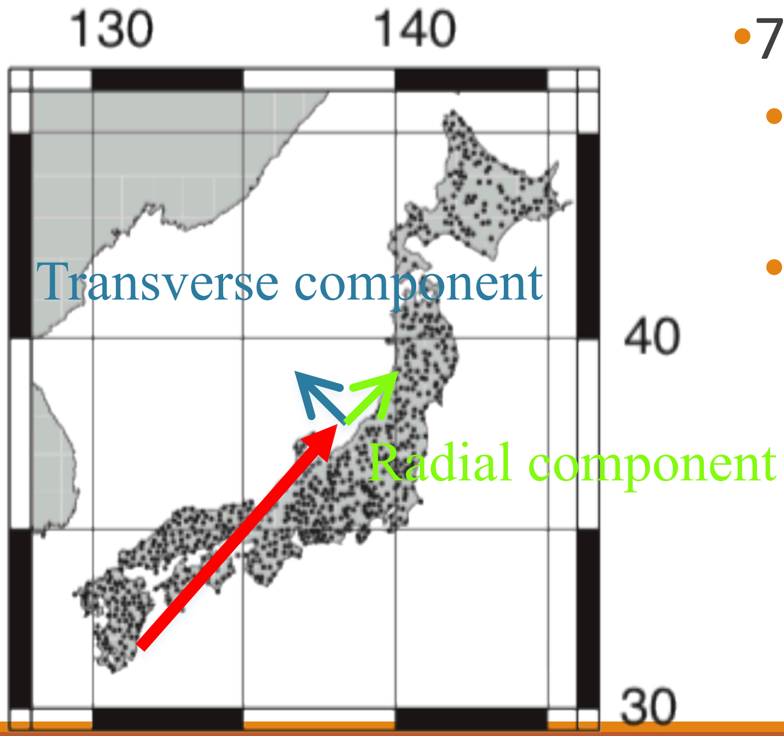

- 775 Hi-net velocitymeters
  - Deconvolution of the response [Maeda et al., 2011]
  - Subtraction of the common logger noise [Takagi et al., 2015]

Teleseismic P and S waves

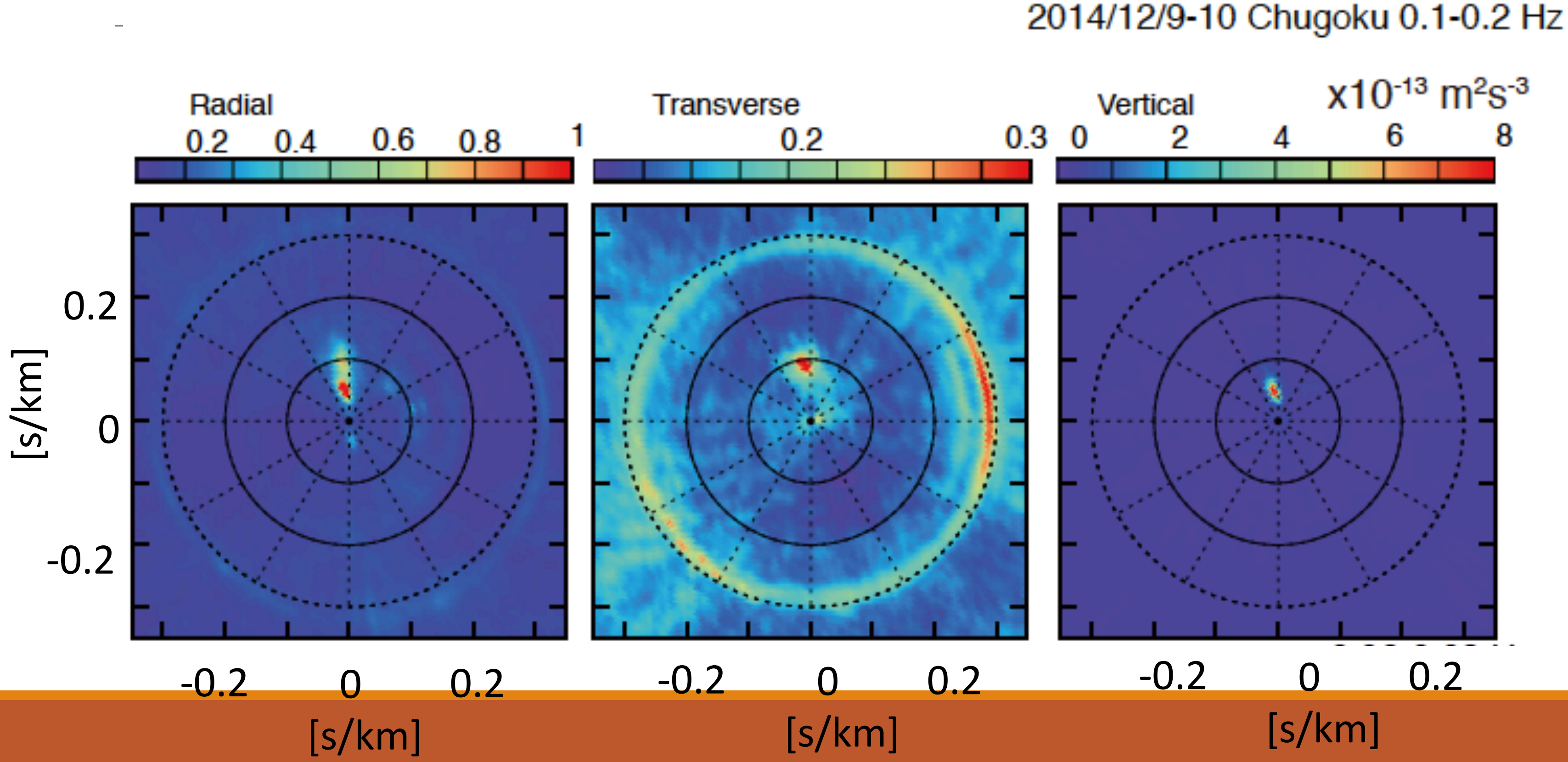

Centroid Single force (CSF)

1. Data: 1024-s segments, Z cmp, 0.1-0.2 Hz
2. Ray theoretical Green's function using IASPEI91 [Gualtieri et al., 2014] with station correction
3. At each grid point (0.1°x0.1°), the source time function was estimated.
4. Centroids were located by picking up the maximum variance reduction.

Locations of the centroids

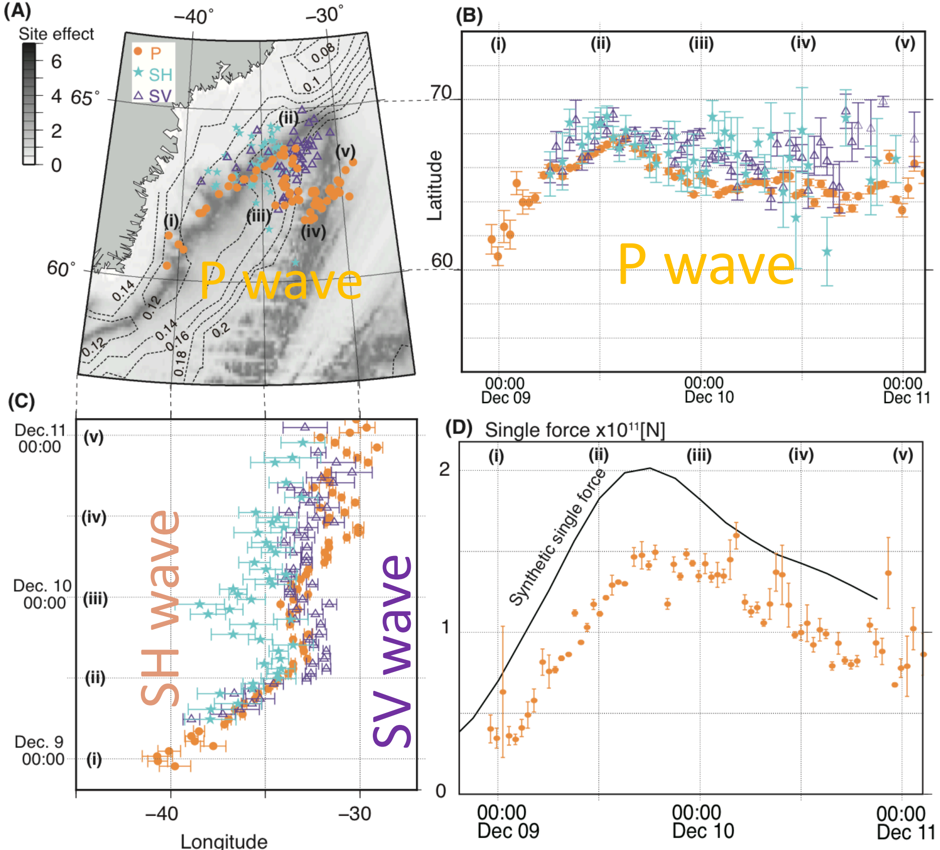

CSF~5x10^{10} [N]

- consistent with wave height model (wave watch III)

Migration of centroids

- East->south->east

SH centroids were located in the thick sediment

- SH&SV (backprojection)

Power spectra of P, SV, and SH waves

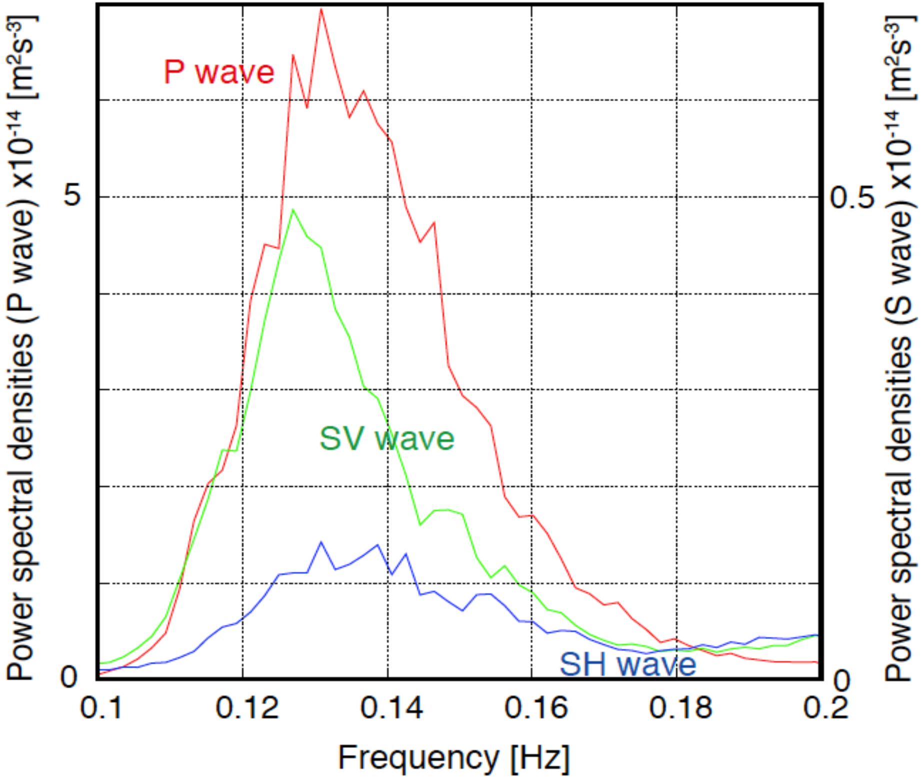

- P ~10xSV,40 xSH in power
- Peak frequency of SH is slightly higher than that of P
- SV converted from P on the ocean floor
- SH: scattering in the sediment?

Origin of S waves

SV-microsiems

- P to SV conversion on the ocean floor can explain observed SV amplitudes [Gualtieri et al. 2014]

SH-wave microseisms

- The sources are located in a coastal region
  - Sudden change of bathymetry, thick sediment
- did not migrate with P-wave microseisms

The observation suggests

- During multiple reflections in the sedimentary layer, S-wave lost polarization information

On a global catalogue of P-wave microseisms (2005-2011) using Hi-net data

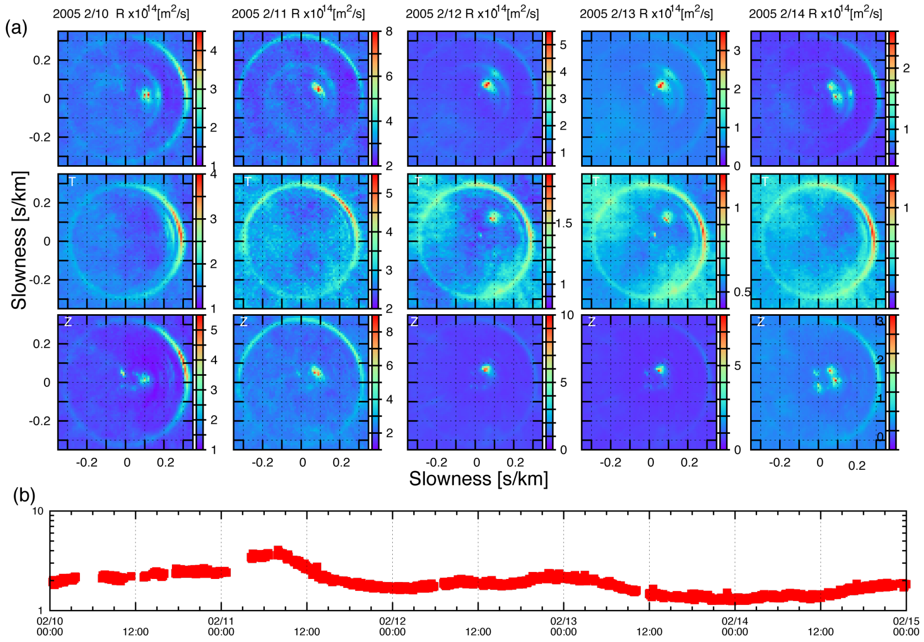

Detection of P-wave microseisms

- 80% of total data
- They are dominant when calm swell activities in local scale
- SH events were rare
  - Several time/year

On seismic exploration beneath a storm

Hypocenters

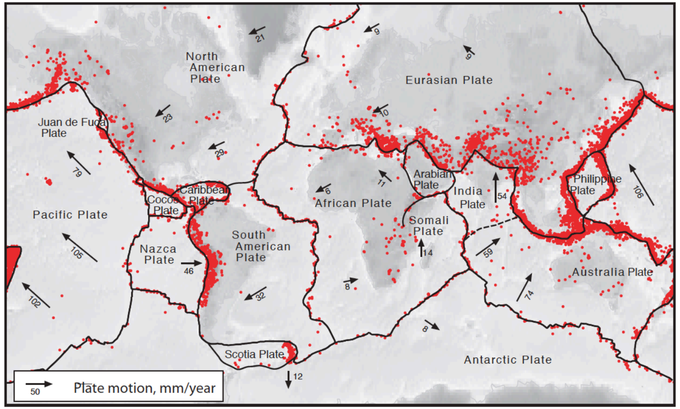

Station distribution

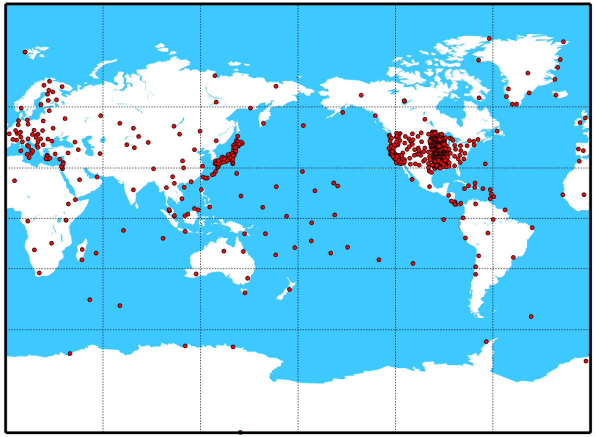

Schematic figure

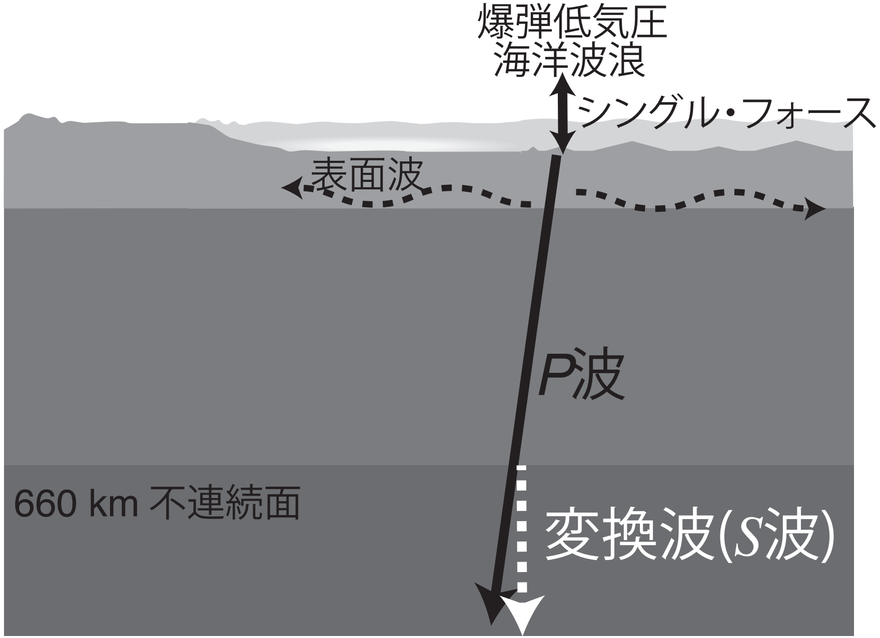

Summary

Detection of P-wave microseims: 80%

- High quality locations: 30%   > 10^{10} N
- consistent with an ocean wave action model

Dominant source areas

- Northwestern Pacific, north Atlantic, southern Indian ocean, arctic sea

New potential sources for exploring the deep Earth.

- Detection of P-SV conversion at 660 km

End

Thank you for your attention